Leader-following distributed control of Multiple Nonholonomic Wheeled Mobile Robot

Lee Zhi Xian*, Muhammad Nasiruddin Mahyuddin*, Guido Herrmann**

***Abstract*— This paper considers leader-following distributed control for nonholonomic mobile agents. The mobile agents consist of a group of wheeled mobile robots with differential drive configurations. With the aid of graph theory, various inter-agent communication scenarios are studied ranging from weakly connected to strongly connected graph. The distributed control scheme defined per agent consists of two levels; one level defines the joint-level velocity control which uses a gradient-based adaptive law to compensate for mobile robot agent dynamics and a sliding-mode control; another level defines the upper level which is responsible for Cartesian control. The consensus algorithm which executes the leader-following protocol resides within the Cartesian control. Several network topologies have been studied by applying the proposed Cooperative Control scheme.**

I. Introduction

Multiple mobile agents working cooperatively pose a greater advantage than a single mobile agent with multiple capabilities. This includes low cost, greater flexibility, adaptability to unknown environments and robustness [1], [2], [3], [4]. Applications such as rescue mission, troop hunting, formation control and rendezvous receive considerable attention [5]. These can be realised by virtue of multiple mobile agents cooperatively controlled by a controller which is distributed rather than centralised. Due to the distributed control architecture, multiple mobile agents are perceived to be flexible and could still perform the prime objective if one of the mobile agents fail. One important issue put forth in coordinating multi-agent systems is to design protocols based only on the local relative information which guarantee consensus reaching by all agent states [6]. Although each agent has limited processing power, the interconnected system as a whole can perform complex tasks in a coordinated fashion [8].

The communication bandwidth and connectivity between agents are often limited. However, with the distributed cooperative control paradigm, each agent will be equipped with simple control law using local neighbouring information to achieve certain prescribed collective behaviours such as maintaining formation, rendezvousing, swarming and reaching consensus [8].

Leader-following consensus problem is a particularly an interesting topic in the field of mobile agents and cooperative control of a networked system. Within a network of coupled mobile agents, only the leader is equipped with information on the specific desired target objective whilst the rest of its corresponding *followers* follow their connected neighbours, oblivious to the actual absolute objective [6]. Leader is a particular agent providing guidance to its follower to steer to the reference input [10]. It was reported that the leader-following configuration is an energy saving mechanism eminent in many biological systems whereby it can enhance the communication and orientation of the flock [9].

Leader-follower cooperative attitude control of multiple rigid bodies was considered in [11] where certain subgroups of the agents is vested in the main control objective, maintaining constant relative orientation amongst themselves.

In this paper, nonholonomic mobile robot is chosen as a platform to illustrate the efficacy of our proposed distributed cooperative control to control a network of mobile agents to follow a leader and maintain certain posture, i.e. the orientation of the mobile robots in the Cartesian coordinate. This paper pays a close attention to the dynamics of a nonholonomic mobile robot as in [12] (for a single-agent robot) both at the joint-space and Cartesian-space level. The multi-agent paradigm from [6], [8] is applied to suit for a multi-robot system.

II. Leader-following Cooperative Control Objective

Let coordinate $[x, y]$ be the coordinate in a Cartesian space for $\mathcal{N}$ agent mobile robots. The cooperative control objective is to be designed is such that

$$lim_{t\to\infty} \begin{bmatrix} \frac{1}{\mathcal{N}} \sum_{i=1}^{\mathcal{N}} x_0 - x_i - x_j = 0 \\ \frac{1}{\mathcal{N}} \sum_{i=1}^{\mathcal{N}} y_0 - y_i - y_j = 0 \end{bmatrix} \quad (1)$$

where $[x_0, y_0]$ refers to the centroid coordinate of the leader agent, $[x_i, y_i]$ refers to the centroid coordinate of the followers and $[x_j, y_j]$ is the respective centroid coordinate of the followers' connected neighbours. (1) represents the leader-following consensus in a multi-agent context. Next, the kinematics and dynamics of each agent mobile robot are to be described.

Lee Zhi Xian is currently a student in the School of Electrical and Electronics Engineering, Universiti Sains Malaysia. Email: zxlee0819@hotmail.com

*Muhammad Nasiruddin Mahyuddin is currently a Senior Lecturer in the School of Electrical and Electronics Engineering, Universiti Sains Malaysia and a Visiting Fellow in the Department of Mechanical Engineering, University of Bristol, BS8 1TR, UK. Email: nasiruddin@usm.my or memnm@bristol.ac.uk

**Guido Herrmann is a Reader in Dynamics and Control with the Department of Mechanical Engineering, University of Bristol, BS8 1TR, UK. Email: g.herrmann@bristol.ac.uk

III. Kinematics and Dynamics of Nonholonomic Wheeled Mobile Robot agent

Consider a multirobot system consisting of $\mathcal{N}$ nonholonomic wheeled mobile robots indexed by $i = 1, 2, \ldots, \mathcal{N}$. A single nonholonomic mobile robot agent is shown in Figure 1. L_i is the half of the wheel separation, R_i is the

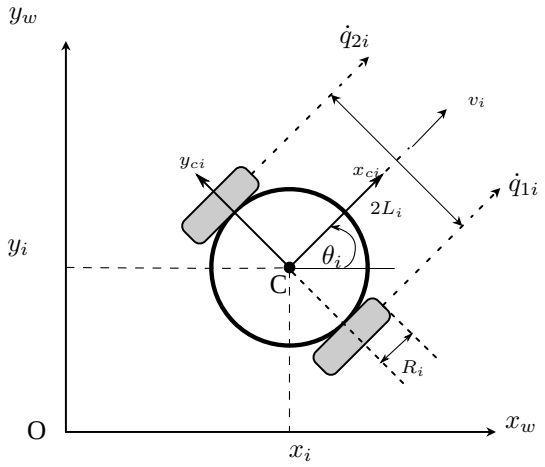

Fig. 1. Configuration of Mobile Robot for each agent.

radius of the wheel, $\dot{q}_{1i}, \dot{q}_{2i}$ are the angular velocity for left and right wheel respectively, θ_i is the robot's orientation A mobile prototype robot constituted by a rigid platform with a differential drive configuration. Two driving wheels are fixed in the front of the platform with same axis of rotation. A third wheel is a free wheel with negligible dynamic effect. The mobile robot is also assumed to traverse a planar flat surface without any elevation satisfying the condition of pure rolling and non-slipping [13] which is to be described in the kinematic section next.

A. Kinematics of each mobile robot agent

The robot motion can be described by the vector $\psi_i = [x_i \ y_i \ \theta_i \ q_{1i} \ q_{2i}]^T \in \mathbb{R}^5$ where (x_i, y_i) is the Cartesian coordinate vector referencing the robot's centroid, θ is the heading of robot and $q_i = [q_{1i} \ q_{2i}]^T$ is the joint space coordinate vector denoting the angular position of the right and left wheels.The pure rolling and non-slipping condition has led to the following relations:

$$-\dot{x}_i cos\theta_i - \dot{y}_i sin\theta_i - L_i\dot{\theta}_i + R_i\dot{q}_{1i} = 0 \quad (2a)$$

$$-\dot{x}_i cos\theta_i - \dot{y}_i sin\theta_i + L_i\dot{\theta}_i + R_i\dot{q}_{2i} = 0 \quad (2b)$$

$$-\dot{x}_i sin\theta_i + \dot{y}_i cos\theta_i = 0 \quad (2c)$$

(2) are the nonholonomic constraints for a differentially-driven mobile robot which must be respected. As subtracting (2a) from (2b) would yield the following solution for obtaining $\theta_i = \theta_{0i} + \frac{R_i}{2L_i}(q_{1i} - q_{2i})$, we can simplify the previous generalised vector ψ_i to $\bar{\psi}_i = [x_i \ y_i \ q_{1i} \ q_{2i}]^T \in \mathbb{R}^4$. It is to verify that these constraints can be represented by a matrix $A_i(\bar{\psi}_i)$,

$$A_i(\bar{\psi}_i)\dot{\bar{\psi}}_i = \begin{bmatrix} -sin\theta_i & cos\theta_i & 0 & 0 \\ -cos\theta_i & -sin\theta_i & \frac{R_i}{2} & \frac{R_i}{2} \end{bmatrix} \begin{bmatrix} \dot{x}_i \\ \dot{y}_i \\ \dot{q}_{1i} \\ \dot{q}_{2i} \end{bmatrix} = 0 \quad (3)$$

Due to the essence and motivation of cooperative control scheme requiring only the mobile robot agent's local information, no external sensor providing absolute position of the robot is needed. Instead, odometry-based computation is employed to obtain the linear velocity v_i and angular velocity of the mobile robot agent ω_i. (2a) and (2b) are added and subtracted together to eliminate the heading term θ yielding,

$$v_i = \frac{R_i}{2}(\dot{q}_{1i} + \dot{q}_{2i}) \quad (4a)$$

$$\omega_i = \frac{R_i}{2L_i}(\dot{q}_{1i} - \dot{q}_{2i}) \quad (4b)$$

Let

$$\mathcal{D}_i = \begin{bmatrix} \frac{R_i}{2} & \frac{R_i}{2} \\ \frac{R_i}{2L_i} & -\frac{R_i}{2L_i} \end{bmatrix} \quad (5)$$

be the matrix that describes the mapping between the angular velocity of the mobile robot's *wheel* ($\dot{q} = [\dot{q}_1 \ \dot{q}_2]$) with the linear and angular velocity of the robot platform $\nu_i = [v_i \ \omega_i]$, then (4) can be equivalently represented as,

$$\nu_i = \mathcal{D}_i\dot{q}_i \quad (6)$$

From the above relation, the velocity of the mobile robot agent in the Cartesian coordinates ($\dot{x} \ \dot{y}$) can be computed simply by using trigonometric relation $\dot{x}_i = v_i cos\theta_i$ and $\dot{y}_i = v_i sin\theta_i$. Then, the following Jacobian matrix $\mathcal{J}(\theta_i)$ can be expressed to describe such relation,

$$\begin{bmatrix} \dot{x}_i \\ \dot{y}_i \\ \dot{\theta}_i \end{bmatrix} = \begin{bmatrix} cos\theta_i & 0 \\ sin\theta_i & 0 \\ 0 & 1 \end{bmatrix} \begin{bmatrix} v_i \\ \omega_i \end{bmatrix} \quad (7)$$

$$\dot{\mathcal{P}}_i = \mathcal{J}_i(\theta_i)\nu_i \quad (8)$$

Note that $\mathcal{P}_i = [x_i \ y_i \ \theta_i]^T$ defines the coordinate vector for each agent in Cartesian space which we want to control. Simply, the solution can be found by

$$\mathcal{P}_i(t) = \mathcal{P}_{0i} + \int_0^t \dot{\mathcal{P}}_i(t)dt \quad (9)$$

$\mathcal{P}_i$ can be also termed as the *posture* of the mobile robot [8]. The mobile robot agent dynamics is to be described next.

B. Dynamic model of mobile robot agent

The dynamic model of the mobile robot i can be described as follows [7], [6], [8].

$$M_i\ddot{q}_i + C_i(q_i, \dot{q}_i)\dot{q}_i + F_{ri}(q_i) + G(q_i) = \tau_i \quad (10)$$

where $q_i = [q_{1i} \ q_{2i}]^T \in \mathbb{R}^{2\times 1}$ is the angular or joint position vector of the wheels of each agent robot, $\dot{q}_i, \ddot{q}_i$ are the vectors of joint velocity and acceleration respectively. $\tau = [\tau_1 \ \tau_2]^T \in$

$\mathbb{R}^{2\times1}$ is the motor torque vector. $M_i \in \mathbb{R}^{2\times2}$ is a symmetric positive definite inertia matrix whose elements can be defined as such,

$$\begin{aligned} M_{i11} &= \frac{R_i^2}{4}m_{pi} + \frac{R_i^2}{4L^2}\mathcal{I}_i + R_i^2 m_{wi} - \frac{R_i^2}{2L_i}m_{pi}\bar{y}_{ci} + \mathcal{I}_{rwi}, \\ M_{i12} &= \frac{R_i^2}{4}m_{pi} - \frac{R_i^2}{4L_i^2}\mathcal{I}_i + \frac{R_i^2}{2}m_{wi}, \\ M_{i22} &= \frac{R_i^2}{4}m_{pi} + \frac{R_i^2}{4L_i^2}\mathcal{I}_i + R_i^2 m_{wi} + \frac{R_i^2}{2L_i}m_{pi}\bar{y}_{ci} + \mathcal{I}_{rwi}, \end{aligned} \tag{11}$$

where $\mathcal{I}_i = \mathcal{I}_{0i} + 2m_{wi}L_i^2 + m_{pi}(\bar{x}_{ci}^2 + \bar{y}_{ci}^2)$ is the moment of inertia of the mobile robot chassis. m_{pi} is the mass of the mobile robot platform including motors, batteries and microcontroller, m_{wi} is the wheel mass, $\bar{x}_{ci}, \bar{y}_{ci}$ are the coordinates of the center of mass of the platform in the mobile frame whilst $\mathcal{I}_{0i}$ is the inertia moment of the platform around the vertical axis passing through its center of mass and $\mathcal{I}_{rwi}$ is the inertia moment of the driving wheel j around its axis of rotation. $C_i(q_i, \dot{q}_i) \in \mathbb{R}^{2\times2}$ is the bounded centripetal and Coriolis matrix containing the following elements,

$$c_{11i} = c_{22i} = 0,\ c_{12i} = -c_{21i} = (\dot{q}_{1i} - \dot{q}_{2i})\frac{R^3}{2L}m_p\bar{y}_c \tag{12}$$

$F_{ri}(\dot{q}_i) \in \mathbb{R}^{2\times1}$ represents the surface friction which can be defined as $F_{ri} = F_v\dot{q}$, $G_i(q_i) \in \mathbb{R}^{2\times1}$ is the gravity vector which can be neglected $G_i(q_i) = 0$ due to non-elevated surface ground.

IV. Inter-agent communication represented by a graph

The inter-agent communication topology between mobile robots is represented by a weighted graph $\mathbb{G} = (\mathbb{V}, \mathbb{E})$ with a vertex set $\mathbb{V} = \{v_1, \ldots, v_\mathcal{N}\}$, an edges set $\mathbb{E} \subseteq \mathbb{V} \times \mathbb{V}$,. An edge of $\mathbb{G}$ is denoted by (i, j) representing that agents i and j can exchange information between them. Two nodes i and j are neighbours to each other if $(i, j) \in \mathbb{E}$. A path is a sequence of connected edges in a graph. A graph is connected if there is a path between every pair of vertices. In this study, we consider four topology cases. Figure 2(a-d) shows the inter-agent communication topology represented by graphs. These graphs can be expressed algebraically by virtue of *adjacency matrix* $\mathcal{A}$. The *adjacency matrix* $\mathcal{A} = (a_{ij})$ is the $n \times n$ symmetric matrix given by $a_{ij} = 1$, if $(i, j) \in \mathbb{E}$ and $a_{ij} = 0$, otherwise. (13) ($\mathcal{A}_1$ (for graph shown in Figure 2a, $\mathcal{A}_2$ (for graph shown in Figure 2b), $\mathcal{A}_3$ (for graph shown in Figure 2c) and $\mathcal{A}_4$ (for graph shown in Figure 2d)) are the algebraic representation that describes the graphs.

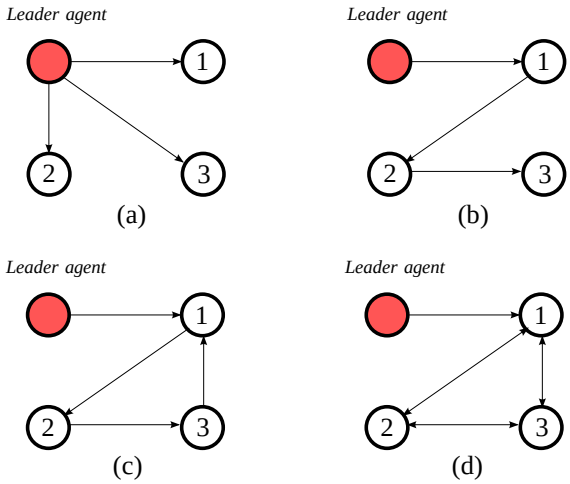

Fig. 2. *Topology 1*: (a) All agents receive information from their leader. *Topology 2*: (b) The topology is connected in a *directed-tree* fashion. *Topology 3*:(c) The subset of Topology 2 except Agent 1 receives information from Agent 3. *Topology 4*:(d) A *strongly*-connected graph or undirected graph.

$$\mathcal{A}_1 = \begin{bmatrix} 0 & 0 & 0 & 0 \\ 1 & 0 & 0 & 0 \\ 1 & 0 & 0 & 0 \\ 1 & 0 & 0 & 0 \end{bmatrix}, \quad \mathcal{A}_2 = \begin{bmatrix} 0 & 0 & 0 & 0 \\ 1 & 0 & 0 & 0 \\ 0 & 1 & 0 & 0 \\ 0 & 0 & 1 & 0 \end{bmatrix}$$
$$\mathcal{A}_3 = \begin{bmatrix} 0 & 0 & 0 & 0 \\ 1 & 0 & 0 & 1 \\ 0 & 1 & 0 & 0 \\ 0 & 0 & 1 & 0 \end{bmatrix}, \quad \mathcal{A}_4 = \begin{bmatrix} 0 & 0 & 0 & 0 \\ 1 & 0 & 1 & 1 \\ 0 & 1 & 0 & 1 \\ 0 & 1 & 1 & 0 \end{bmatrix} \tag{13}$$

V. Cooperative Control of a connected network of mobile robot agents.

The cooperative control strategy proposed is defined at agent level. There are two controllers; joint level controllers will control the motor torque to be applied at robot wheel. The cooperative Cartesian-based controller will control the robot to follow the leader (if they are the *pinned* follower) and/or their connected neighbour agents. The connectivity between agent followers and agent leader has been algebraically expressed by the *adjacency matrix* in (13).

A. Joint-level controller design

Define the error vector,

$$\epsilon_i = \dot{q}_{ci} - \dot{q}_i \tag{14}$$

where $\dot{q}_{ci}$ is the Cartesian controller-generated joint velocity reference for the robot joint velocity $\dot{q}_i$ to follow. To control the joint-tracking of the robot dynamics agent in (10), the following joint-level controller is proposed,

$$\tau_i = \hat{M}_i\dot{\epsilon}_i + \hat{V}_i(q_i, \dot{q}_i)\epsilon_i + \hat{F}_{ri}(\dot{q}_i) + \eta_i + \kappa_i\frac{\epsilon}{|\epsilon|} \tag{15}$$

where $\hat{M}_i$ is the estimated mass matrix, $\hat{V}$ is the estimated Coriolis/cetripetal matrix of mobile robot agent i and $\hat{F}_{ri}$ is

the estimated surface friction on which mobile robot agent i traverses. η_i is defined as,

$$\eta_i = K_{pi}\epsilon + K_{Ii}\int \epsilon dt \tag{16}$$

which can be also viewed as a PI controller. κ_i is the switching gain which amplifies the strength of sliding-mode control employed here for robustification of joint-level control. According to linearity-in-parameter (or LIP) property in [14], the mobile robot dynamic term in (15) can be linearly parameterised,

$$\tau_i = \phi_i(q_i, \dot{q}_i)\hat{\theta}_i + \eta_i + \kappa_i \frac{\epsilon}{|\epsilon|} \tag{17}$$

where $\phi_i(q_i, \dot{q}_i) \in \mathbb{R}^{n\times n}$ is the associated regressor as a function of q_i and $\dot{q}_i$ and n is the degrees of freedom which is 2 in this case. $\hat{\theta}_i \in \mathbb{R}^l$ is the estimated parameter vector (containing l parameters associated with M_i, $C_i(q_i, \dot{q}_i)$ and $F_{ri}(\dot{q}_i)$ in (11) and (12)) which can be estimated by the following gradient-based adaptive law with leakage term,

$$\dot{\hat{\theta}}_i = \Gamma\phi(q_i, \dot{q}_i)\epsilon_i - \hat{\theta}_i \tag{18}$$

The asymptotical convergence of the estimated parameter $\hat{\theta}$ to its true value in (18) is theoretical proven in [16][15] under the condition that the regressor ϕ is Persistently Excited (PE) which can be achieved through a leader reference trajectory being a Sufficiently Rich (SR) signal [17]. The leakage term in (18) stabilizes the adaptive law and preserve certain degree of boundedness as illustrated in [15][16].

Note that, $\dot{q}_{ci}$ (14) in the joint-level controller is computed from the following relation (see (5)),

$$\dot{q}_{ci} = \nu_{ci}\mathcal{D}_i^{-1} \tag{19}$$

Define the following synchronisation error for each agent i,

$$e_{xi} = \sum_{i=1}^{\mathcal{N}} a_{ij}(x_j - x_i) + b_i(x_0 - x_i) \tag{20}$$

$$e_{yi} = \sum_{i=1}^{\mathcal{N}} a_{ij}(y_j - y_i) + b_i(y_0 - y_i) \tag{21}$$

where a_{ij} is the element in the adjacency matrix $\mathcal{A}_i$ defining the connectivity between agents and b_i is the pinning gain. If the follower j receives a direct communication from the leader, then, $b_j = 1$. From the state transformation and trigonometric relation in [7][12], the control input ν_{ci} for each mobile agent is selected as follows

$$\nu_i = \begin{bmatrix} v_{ref}cos(\theta_e) + k_x tanh(e_{xi}) \\ \dot{\theta}_r ef + v_{ref}(k_y tanh(e_{yi}) + k_\theta sin(\theta_e)) \end{bmatrix} \tag{22}$$

where the $tanh(\cdot)$ is the hyperbolic tangent function approximating the signum function. The next section describes the simulation result.

TABLE I
MOBILE ROBOT AGENT PARAMETERS

Parameters (Unit)	Values
M_p(kg)	2.5
M_w(kg)	0.05
(x_c, y_c)(kg)	(0,0)
R(m)	0.2
L(m)	0.62
$I_0(kgm^2)$	0.01
$I_{rw}(kgm^2)$	0.025

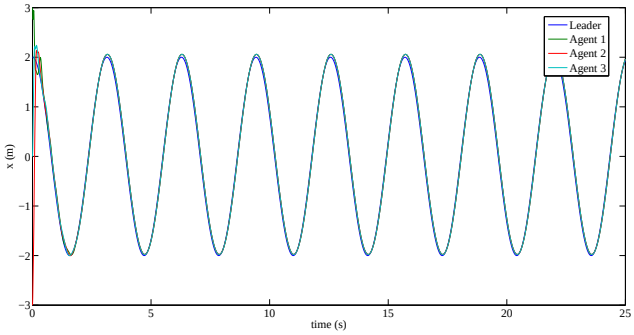

Fig. 3. x_i $\forall$ agent i with respect to the leader's x_0 for case Topology 1.

VI. RESULTS

There are three agents with 1 leader as illustrated in Figure 2a-d. The initial condition of all agents are set as $x_{1_{init}} = [3\ 3\ \pi/2], x_{2_{init}} = [-3\ -3\ \pi/2]$ and $x_{3_{init}} = [0\ 0\ \pi/2]$. The parameters of the mobile robot agents are shown in Table I

For the case of Topology 1, all the mobile robot agents receive full information from the leader and this is equivalent of centralised controller and all the mobile robot agents follow through the leader's trajectory as shown in Figure 3 and Figure 4. Topology 2 illustrates the network of mobile robot agents is in a form of *directed tree* whereby only one of the follower agents is pinned to the leader agent. All the followers agent achieve consensus in following the leader as shown in Figure 5 and Figure 6.

Topology 4 illustrates the full connectivity of all the agent in the network. The graph representing the network can be also called *undirected* as agents communicate in both ways. As shown in Figure 9, Figure 10 and Figure 11, the tracking performance for Topology 4 and Topology 3 are satisfactory and can be further improved by introducing a different nonlinear control design framework, i.e. state transformation (as in ([7])) for Cooperative control.

VII. CONCLUSION

Cooperative control for leader-following of multiple wheeled mobile robot system has been formulated. The control scheme is based on two levels: joint-level control and Cooperative Cartesian-level control. A gradient-based adaptive law with leakage term has been introduced at joint-level to estimate the dynamic parameters of the wheel mobile robot and used for dynamic compensation augmented in

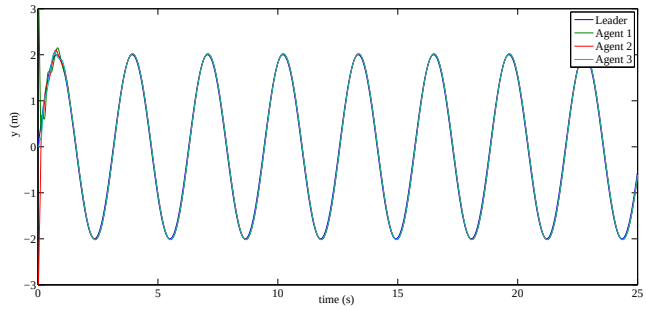

Fig. 4. $y_i \ \forall$ agent i with respect to the leader's y_0 for case Topology 1.

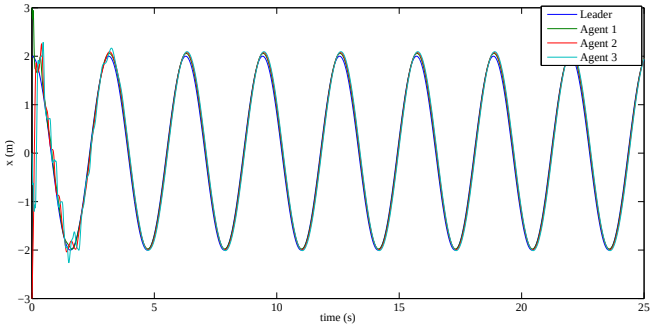

Fig. 5. $x_i \ \forall$ agent i with respect to the leader's x_0 for case Topology 2.

the joint-level control scheme. Robustification term such a signum function is introduced in the joint-level control. The hyperbolic tangent function which is the approximate version of signum function has been introduced in the Cartesian-level, in particular, to force the synchronisation error to zero. All the follower agents achieve a satisfactory consensus whilst following the leader agents for all network topologies studied in this paper.

VIII. Acknowledgement

This work is partially supported by a Fundamental Research Grant Scheme (FRGS) under Grant No. (FRGS-203/PELECT/6071290) awarded by Ministry of Education Malaysia.

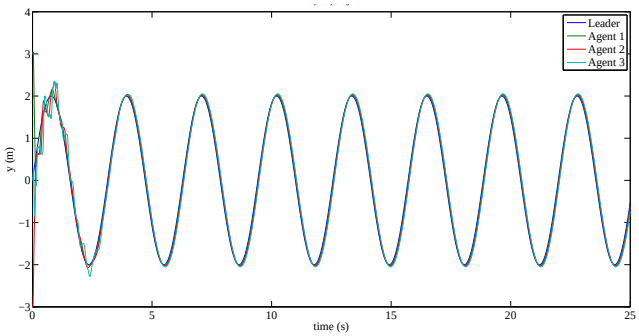

Fig. 6. $y_i \ \forall$ agent i with respect to the leader's y_0 for case Topology 2.

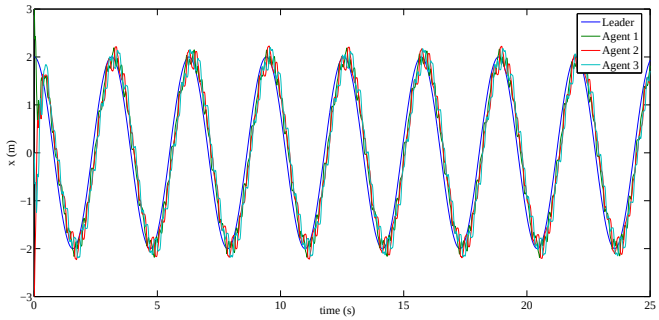

Fig. 7. $x_i \ \forall$ agent i with respect to the leader's x_0 for case Topology 3.

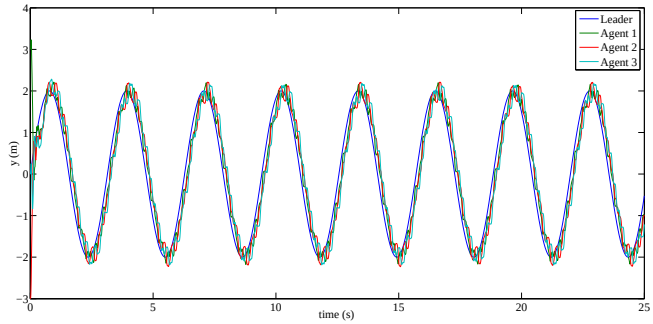

Fig. 8. y_i $\forall$ agent i with respect to the leader's y_0 for case Topology 3.

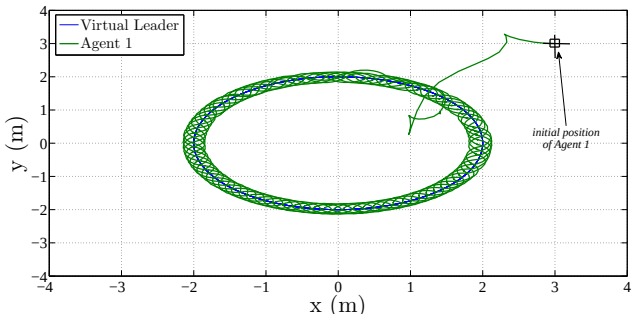

Fig. 9. The phase plot of agent 1 with respect to the leader trajectory for Topology 4 .

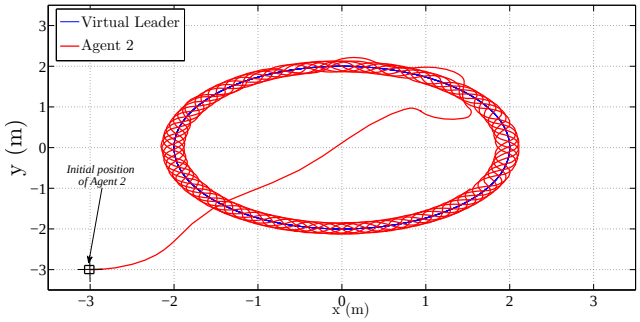

Fig. 10. The phase plot of agent 2 with respect to the leader trajectory for Topology 4 .

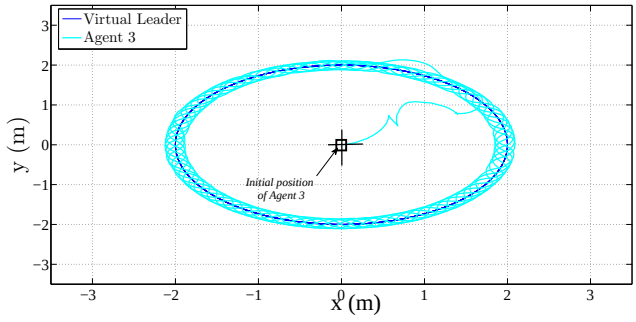

Fig. 11. The phase plot of agent 3 with respect to the leader trajectory for Topology 4 .

REFERENCES

[1] Z. Qu, *Cooperative Control of Dynamical Systems: Applications to Autonomous Vehicles*, Springer, London, UK, 2010.

[2] M. Ghasemi and S.G. Nersesov, "Sliding mode Cooperative control for multi-robot systems: a finite-time approach," *Mathematical Problems in Engineering*, vol. 2013, Article ID 450201, 16 pages, 2013.

[3] H.G. Tanner and J.L. Piovesan, "Randomized receding horizon navigation," *IEEE Transactions on Automatic Control*, vol. 55, no. 11, pp. 2640-2644, 2010.

[4] M. Lei, S. Zhou and G. Yin, "Complex formation control of large-scale intelligent autonomous vehicles," *Mathematical Problems in Engineering*, vol. 2012, Article ID 241916, 19 pages, 2012.

[5] W. Dong and J. A. Farrell, "Cooperative Control of Multiple Nonholonomic Mobile Agents," *IEEE Transactions on Automatic Control*, 2008.

[6] W. Ren, R.W. Beard and E.M. Atkin, "Information consensus in multivehicle cooperative control: collective group behaviour through local interaction," *IEEE Control System Magazine*, 2007, 27(2):71-82.

[7] Z. Peng, S. Yang, G. Wen and A. Rahmani, "Distributed Consensus-Based Robust Adaptive Formation Control for Nonholonomic Mobile Robots with Partial Known Dynamics" *Mathematical Problems in Engineering*, vol. 2014, Article ID 670497, 12 pages, 2014.

[8] W. Ni, and D. Cheng, "Leader-following consensus of multi-agent systems under fixed and switching topologies" *System and Control Letters*, vol.59, 2010, pp. 209–217.

[9] M. Andersson, J. Wallander, "Kin Selection and reciprocity in flight formation" *Behavioural Ecology* 15(1)(2004) pp. 158-162.

[10] B. Liu, T. Chu, L. Wang, and G. Xie, "Controllability of a leader-follower dynamic network with switching topology," *IEEE Transaction on Automatic Control* 53 (4) (2008) pp. 1009-1013.

[11] , "Leader-follower cooperative attitude control of multipled rigid bodies," *Systems and Control Letters* 58 (2009) pp. 429-435.

[12] D.V. Dimarogonas, P. Tsiotras and K.J. Jyriakopolous, "Dynamic Control of Nonholonmic Mobile Robot in Cartesian Space," in *Decision and Control, 1995, Proceedings of the 34th IEEE Conference on*, dec. 1995, pp. 3825 – 3830.

[13] R. Fierro and F.L. Lewis, "Control of a Nonholonomic Mobile Robot: Backstepping Kinematics into Dynamics," in *Decision and Control, 1995, Proceedings of the 34th IEEE Conference on*, dec. 1995, pp. 3805 – 3810.

[14] F.L. Lewis, D.M. Dawson, and C.T. Abdallah, "*Robot Manipulator Control: Theory and Practise*", Marcel Dekker, 2004.

[15] K. Narendra and A. Annaswamy, "*Stable Adaptiv Systems*", Dover Publications, 2012.

[16] P. Ioannou and J. Sun, "*Robust Adaptive Control*", Prentice Hall, 1996.

[17] M.N. Mahyuddin, G. Herrmann, J. Na and F.L. Lewis, "Finite-time adaptive distributed control for double integrator leader-agent synchronisation", in *Intelligent Control (ISIC), 2012 IEEE International Symposium on*, oct. 2012, pp. 714-720.